23. Espada-Murao LA, Morita K: **Delayed cytosolic exposure of Japanese encephalitis virus double-stranded RNA impedes interferon activation and enhances viral dissemination in porcine cells.** *J Virol* 2011, **85**:6736–6749.
24. Oberste MS, Maher K, Kennett ML, Campbell JJ, Carpenter MS, Schnurr D, Pallansch MA: **Molecular epidemiology and genetic diversity of echovirus type 30 (E30): genotypes correlate with temporal dynamics of E30 isolation.** *J Clin Microbiol* 1999, **37**:3928–3933.
25. Hayasaka D, Gritsun TS, Yoshii K, Ueki T, Goto A, Mizutani T, Kariwa H, Iwasaki T, Gould EA, Takashima I: **Amino acid changes responsible for attenuation of virus neurovirulence in an infectious cDNA clone of the oshima strain of tick-borne encephalitis virus.** *J Gen Virol* 2004, **85**:1007–1018.
26. Larkin MA, Blackshields G, Brown NP, Chenna R, McGettigan PA, McWilliam H, Valentin F, Wallace IM, Wilm A, Lopez R, *et al*: **Clustal W and clustal X version 2.0.** *Bioinformatics* 2007, **23**:2947–2948.
27. Tamura K, Nei M: **Estimation of the number of nucleotide substitutions in the control region of mitochondrial DNA in humans and chimpanzees.** *Mol Biol Evol* 1993, **10**:512–526.
28. Tamura K, Peterson D, Peterson N, Stecher G, Nei M, Kumar S: **MEGA5: molecular evolutionary genetics analysis using maximum likelihood, evolutionary distance, and maximum parsimony methods.** *Mol Biol Evol* 2011, **28**:2731–2739.
29. Ihaka R, Gentleman R: **R: a language for data analysis and graphics.** *J Comput Graph Stat* 1996, **5**:299–314.
30. Shoji H, Hiraki Y, Kuwasaki N, Toyomasu T, Kaji M, Okudera T: **Japanese encephalitis in the Kurume region of Japan: CT and MRI findings.** *J Neurol* 1989, **236**:255–259.
31. Kalita J, Misra UK: **Comparison of CT scan and MRI findings in the diagnosis of Japanese encephalitis.** *J Neurol Sci* 2000, **174**:3–8.
32. Ayukawa R, Fujimoto H, Ayabe M, Shoji H, Matsui R, Iwata Y, Fukuda H, Ochi K, Noda K, Ono Y, *et al*: **An unexpected outbreak of Japanese encephalitis in the Chugoku district of Japan, 2002.** *Jpn J Infect Dis* 2004, **57**:63–66.
33. Wong KT, Ng KY, Ong KC, Ng WF, Shankar SK, Mahadevan A, Radotra B, Su IJ, Lau G, Ling AE, *et al*: **Enterovirus 71 encephalomyelitis and Japanese encephalitis can be distinguished by topographic distribution of inflammation and specific intraneuronal detection of viral antigen and RNA.** *Neuropathol Appl Neurobiol* 2012, **38**:443–453.
34. Martinez AA, Castillo J, Sanchez MC, Zaldivar Y, Mendoza Y, Tribaldos M, Acosta P, Smith RE, Pascale JM: **Molecular diagnosis of echovirus 30 as the etiological agent in an outbreak of aseptic meningitis in Panama: May - June 2008.** *J Infect Dev Ctries* 2012, **6**:836–841.
35. Mantadakis E, Pogka V, Voulgari-Kokota A, Tsouvala E, Emmanouil M, Kremastinou J, Chatzimichael A, Mentis A: **Echovirus 30 outbreak associated with a high meningitis attack rate in Thrace, Greece.** *Pediatr Infect Dis J* 2013, **32**:914–916.

doi:10.1186/1743-422X-10-280
Cite this article as: Takamatsu *et al.*: An approach for differentiating echovirus 30 and Japanese encephalitis virus infections in acute meningitis/encephalitis: a retrospective study of 103 cases in Vietnam. *Virology Journal* 2013 **10**:280.

Journal of General Virology (2014), **95**, 373–383 DOI 10.1099/vir.0.057968-0

NS1′ protein expression facilitates production of Japanese encephalitis virus in avian cells and embryonated chicken eggs

Yuki Takamatsu,[1,2] Kenta Okamoto,[1] Duc Tuan Dinh,[1,3] Fuxun Yu,[1] Daisuke Hayasaka,[1] Leo Uchida,[1,2] Takeshi Nabeshima,[1] Corazon C. Buerano[1,4] and Kouichi Morita[1]

Correspondence
Kouichi Morita
moritak@nagasaki-u.ac.jp

[1]Department of Virology, Institute of Tropical Medicine (NEKKEN), Nagasaki University, Nagasaki, Japan

[2]Graduate School of Biomedical Sciences, Nagasaki University, Nagasaki, Japan

[3]Respiratory Viruses Laboratory, Department of Virology, National Institute of Hygiene and Epidemiology, Hanoi, Vietnam

[4]Department of Molecular Epidemiology, Institute of Tropical Medicine (NEKKEN), Nagasaki University, Nagasaki, Japan

Japanese encephalitis virus (JEV), which belongs to the genus *Flavivirus* of the family *Flaviviridae*, is a leading cause of meningo-encephalitis in Asian countries. The flavivirus non-structural protein 1 (NS1) plays a role in virus replication and in the elicitation of an immune response. The NS1′ protein found among the members of the JEV subgroup is an extended form of NS1 and is generated by a −1 ribosomal frameshift. This protein is known to be involved in viral pathogenicity; however, its specific function is still unknown. Here, we describe an investigation of the molecular function of NS1′ protein through the production of JEV NS1′-expressing and -non-expressing clones and their infection of avian and mammalian cells. Efficient NS1′ protein expression was observed in avian cells and was found to facilitate JEV production in both avian cultured cells and embryonated chicken eggs. NS1′ protein was observed to co-localize with NS5 protein and resulted in increased viral RNA levels in avian cells. These findings clearly indicate that NS1′ enhances the production of JEV in avian cells and may facilitate the amplification/maintenance role of birds in the virus transmission cycle in nature.

Received 5 August 2013
Accepted 28 October 2013

INTRODUCTION

Japanese encephalitis virus (JEV), which is transmitted among birds, pigs and *Culex* mosquitoes, causes about 30 000–50 000 meningo-encephalitis cases and 10 000–15 000 deaths in Asian countries annually (Ghosh & Basu, 2009; Solomon, 2004). Reservoir hosts play a central role in virus ecology by being viraemic and available within the immediate vector flight range. Wading birds using the rice-cultivated surface provide a high availability of resources to mosquito vectors by enhancing JEV maintenance, amplification and transmission (Le Flohic *et al.*, 2013). JEV belongs to the family *Flaviviridae*, genus *Flavivirus* (Westaway *et al.*, 1985). The flavivirus genome is a non-segmented 11 kb positive-sense RNA that encodes three structural (C, prM and E) and seven non-structural (NS1, NS2A, NS2B, NS3, NS4A, NS4B and NS5) proteins (Lindenbach & Rice, 1997; Sumiyoshi *et al.*, 1992). The NS1 protein, which co-localizes with the dsRNA in a replication complex (MacKenzie *et al.*, 1996), is required for the initial negative-strand RNA synthesis (Lindenbach & Rice, 1997). Its secreted form plays a role in modulation of the host immune response (Chung *et al.*, 2006b, 2007; Lin *et al.*, 1998; Wilson *et al.*, 2008), and regulates the host complementary system by interacting with several complementary factors, such as fH, C3b and C4 proteins (Avirutnan *et al.*, 2010; Chung *et al.*, 2006a; Ferreira *et al.*, 2010; Schlesinger, 2006).

The NS1′ protein (55 kDa, glycosylated) has been detected among members of a JEV subgroup including West Nile virus (WNV) and Murray Valley encephalitis virus (MVEV) (Blitvich *et al.*, 1995; Chen *et al.*, 1996; Lin *et al.*, 1998; Mason, 1989). This protein is produced as a result of a −1 ribosomal frameshift at the conserved slippery heptanucleotide (YCCUUUU) and 3′-adjacent potential pseudoknot near the beginning of the NS2A-coding

Three supplementary tables and five figures are available with the online version of this paper.

gene (Firth & Atkins, 2009). There are reports that NS1′ plays an important role in the increased virulence of WNV and JEV (Melian *et al.*, 2010; Ye *et al.*, 2012). A recent report showed that NS1′ co-localizes with NS1 and substitutes for NS1 in WNV replication (Young *et al.*, 2013). Flaviviruses expressing NS1′ have been suggested to have been evolutionarily selected for an advantage in virus replication/transmission in the mosquito–host cycle (Melian *et al.*, 2010).

The present study focused on the JEV NS1′ protein and on the elucidation of its molecular function(s), especially in avian cells. Our study showed that a mutation at nt 67 in the NS2A-coding region of JEV was critical for NS1′ production. We have revealed that the NS1′ protein facilitated JEV production in avian cells based on the increasing viral RNA level. This protein was found to co-localize efficiently with cytoplasmic NS5 protein (an RNA-dependent RNA polymerase) in avian cells. *In vivo*, NS1′ expression enhanced virus production and increased mortality in embryonated chicken eggs (ECEs). These results suggest a novel fundamental role of the NS1′ protein in avian cells by influencing efficient survival of JEV in the natural transmission cycle through the facilitation of virus production in these cells.

RESULTS

NS2A G67A mutation abolishes NS1′ protein production

Two JEV infectious clones (ICs), S982-IC and JaTH-IC, used in this study differed in expressing NS1′ in mammalian (BHK) and avian (DF-1) cells. S982-IC did not express NS1′ in these vertebrate cells but expressed NS1 protein, whereas JaTH-IC expressed both NS1′ and NS1 proteins in these cells (Fig. 1a). In S982-IC, an A was present at nt 67 of the *NS2A* gene, whereas JaTH-IC had a G in this position instead (Figs 1b and S1a, available in JGV Online). Analysis of the RNA secondary structure of this gene predicted that this nucleotide change disrupted the pseudoknot structure, which was critical for the −1 ribosomal frameshifting (Fig. S1b). A point mutation was introduced at nt 67 in the *NS2A* gene of the two clones as described in Methods, and the constructed ICs were designated S982-A67G-IC, which was able to produce NS1 and NS1′ proteins, and JaTH-G67A-IC, which produced NS1 but not NS1′ proteins as expected (Fig. 1c). These results indicated that the G at position 67 in NS2A coding region plays a critical role in production of the NS1′ protein. The G67A mutation resulted in a V23I amino acid mutation in the NS2A protein. In order to eliminate the influence of the amino acid change from I to V at position 23 of NS2A, JaTH-G66A-IC was developed. JaTH-G66A-IC produced NS1 but not NS1′ proteins as expected (Fig. 1c). A description of the original ICs and mutated clones with respect to nucleotide and amino acid differences and NS1′ expression is given in Table S1.

Expression levels of NS1′ protein in DF-1 and BHK cells

NS1′ expression by JEV ICs in avian cells (DF-1) was compared with that in mammalian cells (BHK) at 48 h post-infection (p.i.). The bands for the NS1′ protein showed a four- to fivefold greater intensity compared with those of the NS1 protein in the DF-1 cells infected with NS1′-expressing viruses (S982-A67G-IC and JaTH-IC). In contrast, bands of similar intensity were observed for the NS1′ and NS1 proteins in BHK cells infected with the same viruses (Fig. 1c).

NS1′ protein expression facilitates virus production in avian cells

Some noteworthy findings arose after comparing the growth characteristics of the ICs in BHK and DF-1 cells (Fig. 2). Foci of similar size were formed in BHK cells that were infected with any of the ICs (Fig. 2a); however, larger foci were formed in avian DF-1 cells when infected with the NS1′-expressing viruses (Fig. 2b).

Growth curves showed that the titres of the NS1′-expressing viruses were over 10 times higher than those of the NS1′-non-expressing viruses (S982-IC, JaTH-G67A-IC and JaTH-G66A-IC) at 48 and 72 h p.i. in DF-1 cells (Fig. 2c); however, all of the ICs showed almost equal titres in BHK cells. These results indicated that NS1′ expression can enhance virus propagation in avian cells.

NS1′ protein co-localizes with NS5 protein

NS1′-specific polyclonal antibodies were produced as described in Methods. These antibodies were found to detect only NS1′ in cells infected with the NS1′-expressing viruses by Western blotting and immunofluorescent staining (Fig. 3a, b). In contrast, the anti-NS1 antibodies could not discriminate between the NS1 and NS1′ proteins (Fig. 3b). With the application of anti-NS1′ antibodies and anti-NS5 antibodies, NS1′ proteins were found to co-localize with NS5 proteins in BHK and DF-1 cells that were infected with the NS1′-expressing viruses (Fig. 4). This co-localization was observed at 12 h p.i. and increased over time (data not shown).

NS1′ protein efficiently interacts with NS5 protein in avian cells

A higher co-localization rate of NS1′ and NS5 in DF-1 cells was noted by confocal laser-scanning microscopy analysis. A 20–30 % co-localization of NS1′ and NS5 was observed in BHK cells infected with the NS1′-expressing viruses, whereas 60–70 % was observed in DF-1 cells infected with the same viruses (Fig. 4).

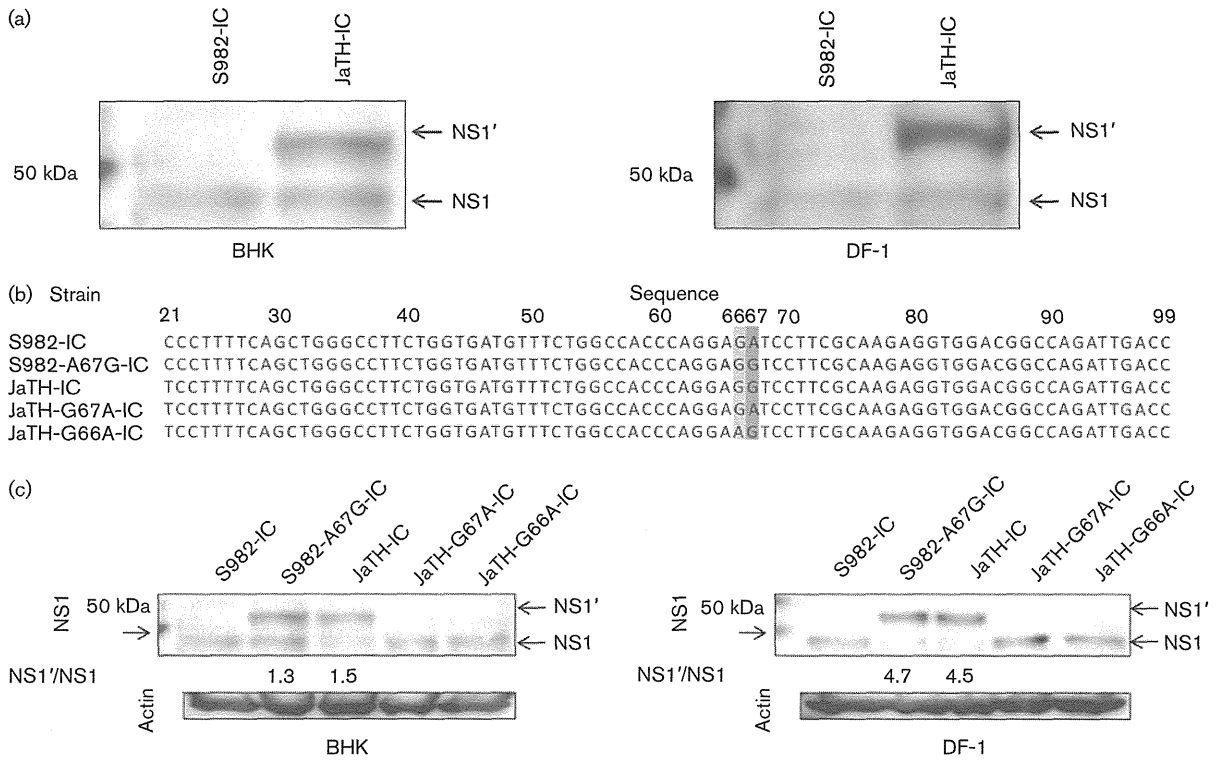

Fig. 1. NS1′ expression and alignment of nucleotide sequences of the studied viruses. (a) Detection of NS1 and NS1′ in JEV-infected cells. BHK and DF-1 cells were infected at an m.o.i. of 10 for 48 h with S982-IC or JaTH-IC. Cellular extracts were subjected to Western blotting with JEV anti-NS1 polyclonal antibodies. (b) Alignment of nucleotide sequences in the NS2A gene of the five viruses used in this study. The number above the sequence indicates nucleotide position in the NS2A gene. The nucleotides at positions 66 and 67 of the NS2A gene are highlighted in light grey and dark grey, respectively. Alignment of the NS2A gene showed that JaTH-G66A-IC had an A at position 66, and S982-IC and JaTH-G67A-IC had an A at position 67 of NS2A gene. (c) Detection of NS1 and NS1′ in BHK and DF-1 cells infected with the indicated viruses at an m.o.i. of 10 for 48 h. Cellular extracts were subjected to Western blotting for the detection of proteins indicated on the left side of the figure, with β-Actin as the internal control. The number below a band lane indicates relative intensity of NS1′ band divided by the intensity of NS1 band.

Co-immunoprecipitation (Co-IP) by purified anti-NS1 or anti-NS5 antibodies resulted in the co-precipitation of NS5 and NS1/NS1′ in the lysates of BHK and DF-1 cells infected with JEV ICs (Fig. 5a, b). The NS5 protein levels in DF-1 cells infected with the NS1′-expressing viruses were 1.8–2.2 times higher in comparison with those infected with the NS1′-non-expressing viruses when they were co-precipitated by the anti-NS1 antibodies (Fig. 5a). In contrast, in BHK cells infected with all the studied viruses, a similar amount of co-precipitated NS5 proteins was observed (Fig. 5a). A similar amount of NS1 proteins was observed in BHK and DF-1 cells when they were co-precipitated by the anti-NS5 antibodies (Fig. 5b). However, NS1′ protein levels in DF-1 cells infected with the NS1′-expressing viruses were three to four times higher in comparison with those in BHK cells that were infected with the same viruses (Fig. 5b). These results suggested that NS1′ proteins can directly or indirectly interact with NS5 proteins as well as with NS1 proteins, and that this interaction is highly efficient in avian DF-1 cells.

NS1′ protein increases viral RNA levels in avian cells

Real-time quantitative reverse transcription (RT)-PCR analysis revealed that the NS1′ protein expression significantly upregulated viral RNA copy number in DF-1 cells but not in BHK cells (Fig. 6). The viral RNA level was 10 times higher in the NS1′-expressing viruses when compared with that in the NS1′-non-expressing viruses from 12 up to 72 h p.i. in DF-1 cells (Fig. 6b). A significant difference in RNA copy number was observed between S982-IC and S982-A67G-IC at 24, 36, 48 and 72 h p.i. in DF-1 cells (Fig. 6b). A significant difference in RNA copy number was also observed between JaTH-IC and JaTH-G67A-IC at 24, 36 and 72 h p.i. in DF-1 cells. In addition, a significant difference in RNA copy number was observed between JaTH-IC and JaTH-G66A-IC at 12, 24, 36, 48 and 72 h p.i. in DF-1 cells (Fig. 6b). In contrast, RNA level was not significantly different among the studied viruses in BHK

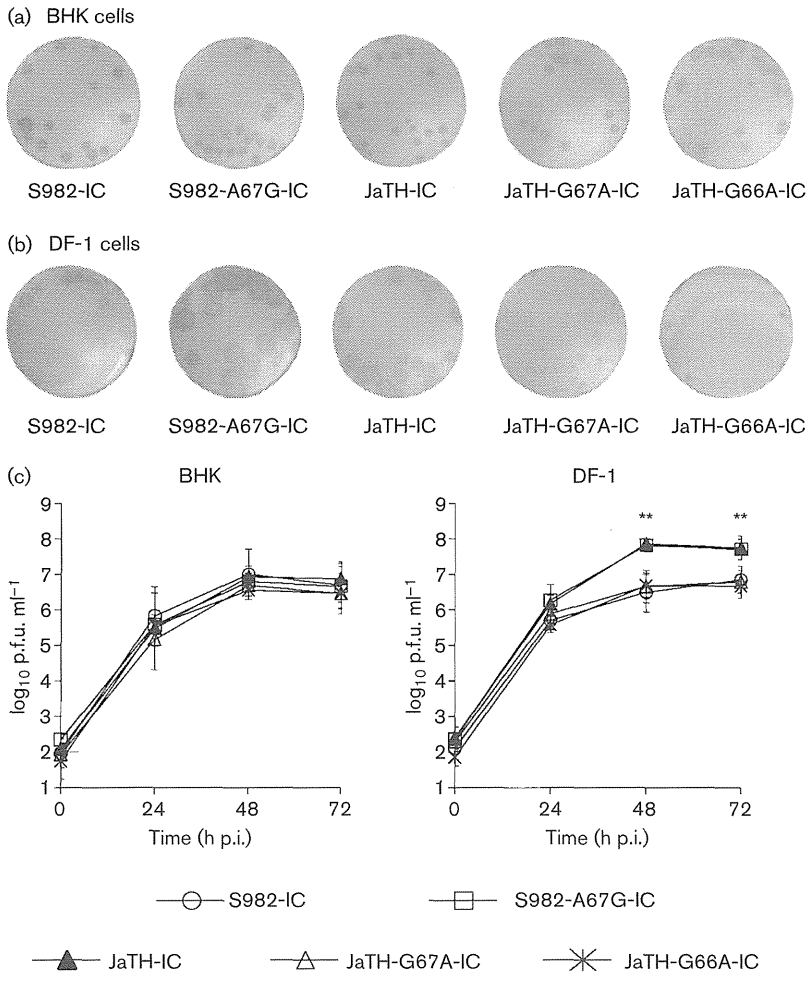

Fig. 2. Focus formation and growth curves in BHK and DF-1 cells. (a, b) BHK (a) and DF-1 (b) cells were infected with the indicated viruses, and differences in focus morphology caused by these viruses were compared on day 3 p.i. (c) Titres of virus from the supernatants of cells infected with the ICs (m.o.i. 0.1) were measured at the indicated times p.i. The values among groups were tested by one-way ANOVA analysis. Statistically significant differences in titres between the NS1′-expressing viruses (S982-A67G-IC and JaTH-IC) and the NS1′-non-expressing viruses (S982-IC, JaTH-G67A-IC and JaTH-G66A-IC) are indicated (**$P<0.01$). Results are expressed as means ± SD from three independent experiments.

cells (Fig. 6a). It was concluded that NS1′ protein expression enhanced viral RNA level only in avian cells.

NS1′ protein increases virus production and mortality in ECEs

There are some studies on the use of ECEs as a flavivirus infection model (Crespo *et al.*, 2009; Osorio *et al.*, 2012). Survival curves of ECEs infected with the NS1′-expressing and NS1′-non-expressing viruses were compared to reveal the influence of NS1′ expression. The survival curves showed that the NS1′-expressing viruses at a dose of both 10^4 and 10^2 p.f.u. per egg killed all ECEs by 6–9 days post-inoculation (Fig. 7a, b). In contrast, infection of ECEs with the NS1′-non-expressing viruses at a dose of 10^4 and 10^2 p.f.u. per egg resulted in a mortality of 80–100 % (S982-IC, 100 %; JaTH-G67A-IC, 80 %; JaTH-G66A-IC, 80 %; Fig. 7a) and 40–70 % (S982-IC, 70 %; JaTH-G67A-IC, 50 %; JaTH-G66A-IC, 40 %; Fig. 7b), respectively. All the viruses studied in this paper showed 100 % mortality in ECEs after inoculation of 10^5 p.f.u. per egg (data not shown).

On day 5 after inoculation of 10^4 p.f.u. per egg, embryonic tissues and yolk sac tissues from live and dead ECEs were collected and the recovered virus titres were compared. A significant increase in virus titre was observed in both embryonic and yolk sac tissues infected with the NS1′-expressing viruses (Fig. 7c, d). No significant difference in virus amount was observed in the tissues taken from live ECEs and from the dead ECEs infected with the same virus for both the NS1′-expressing and NS1′-non-expressing viruses. In 7-day-old ECEs, it was difficult to distinguish each organ, and no significant difference in virus amount was observed between embryo tissues and yolk sac tissues in each infected ECEs (Fig. S2a). In 14-day-old ECEs, tissue tropism was compared between the NS1′-expressing virus JaTH-IC and the NS1′-non-expressing virus JaTH-G66A-IC (Fig. S2b). The titre of virus in each tissue/organ infected with the NS1′-expressing virus was relatively higher than that infected with the NS1′-non-expressing virus. A significant difference between the two viruses was observed only in the liver (Fig. S2c).

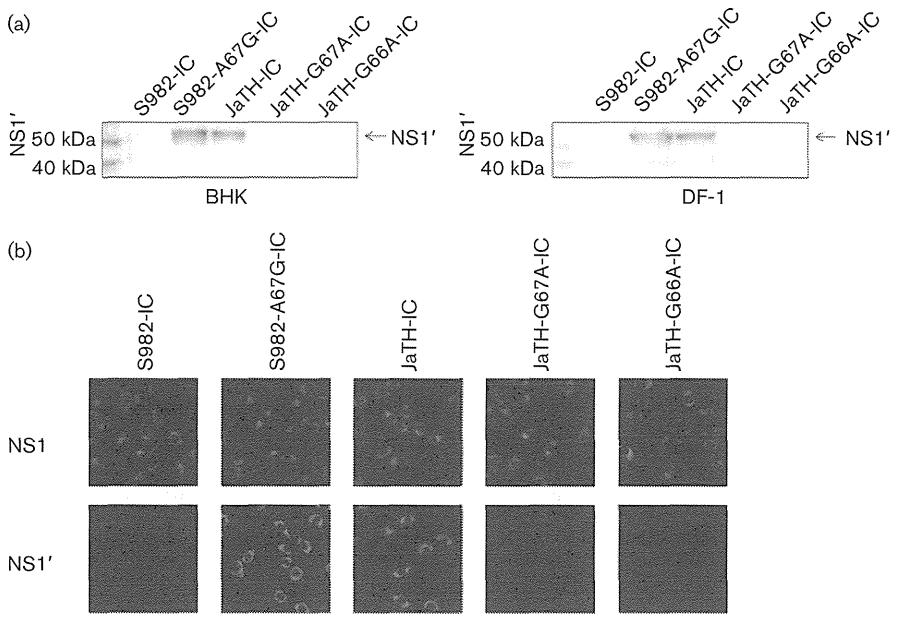

Fig. 3. Specificity of NS1′ antibodies. (a) The specificity of antibodies against NS1′ protein was confirmed by Western blotting. BHK and DF-1 cells were infected with each virus at an m.o.i. of 10. Western blotting was carried out on the extracted proteins and NS1′-specific polyclonal antibodies produced as described in Methods were used as detecting antibodies. (b) Subcellular localization of NS1 and/or NS1′ was observed in BHK cells. Anti-NS1 or anti-NS1′ antibodies were used as primary antibodies, and Alexa Fluor 568-conjugated anti-mouse antibodies were used for secondary labelling. The anti-NS1 antibodies detected NS1 and NS1′ in all five viruses, whereas the anti-NS1′ antibodies detected NS1′ only in the NS1′-expressing viruses.

DISCUSSION

Although there are a number of reports on the roles of NS1 in virus replication (Khromykh *et al.*, 1999; Lindenbach & Rice, 1997, 1999; MacKenzie *et al.*, 1996; Muylaert *et al.*, 1996; Youn *et al.*, 2012), only a few reports have dealt with the function(s) of NS1′. These reports on NS1′ have suggested that this protein has no critical effect on virus

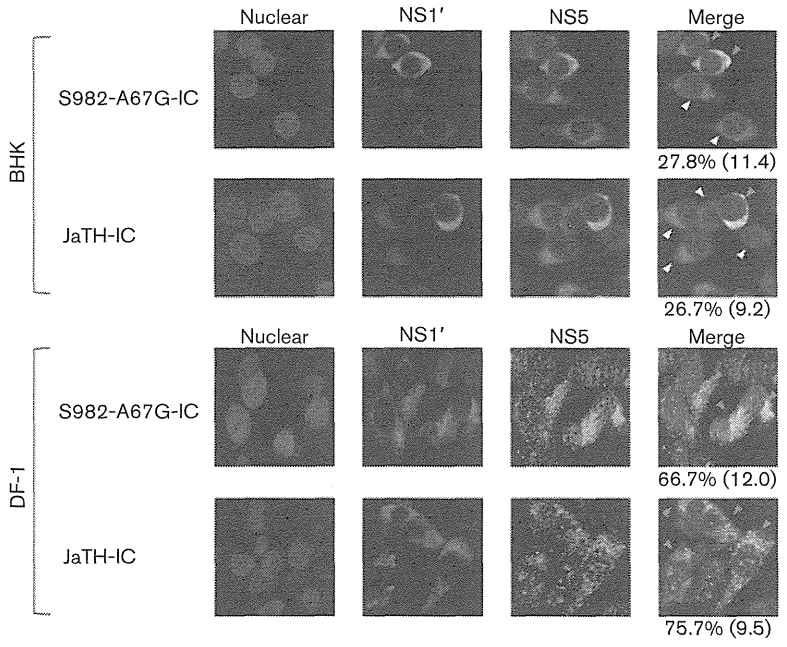

Fig. 4. Subcellular co-localization of NS1′ with NS5 in BHK and DF-1 cells. BHK and DF-1 cells were infected with the NS1′-expressing viruses (S982-A67G-IC and JaTH-IC) at an m.o.i. of 10, and the subcellular localization of NS1′ and NS5 was compared at 48 h p.i. Nuclear staining was achieved using DAPI. The number shown below the merged image indicates the co-localization percentage of NS1′ and NS5 signals. The percentage was calculated as the number of NS1′ and NS5 double-positive cells (red arrowheads) divided by the number of NS5-positive cells (white arrowheads) and is shown as the mean value from ten fields with SD indicated in parentheses.

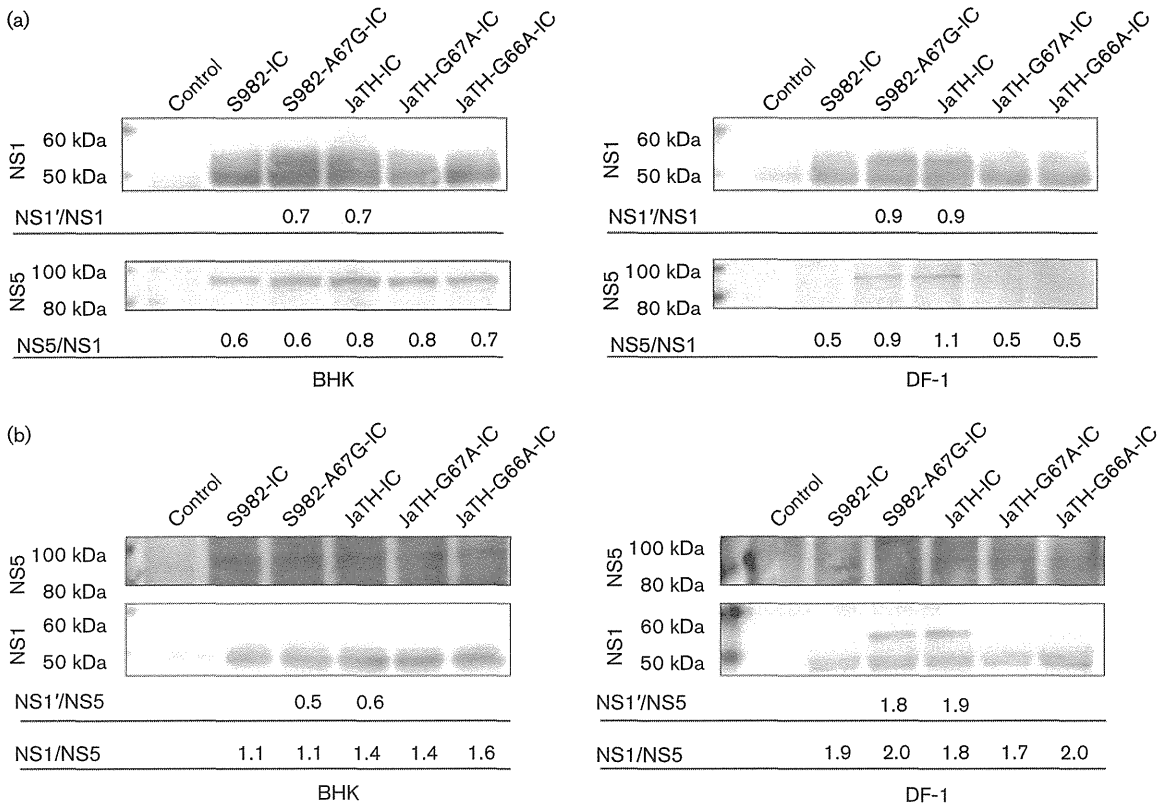

Fig. 5. Co-IP of NS1′ and NS5. (a) BHK and DF-1 cells were infected with S982-IC, S982-A67G-IC, JaTH-IC, JaTH-G67A-IC or JaTH-G66A-IC. PBS was used as a control. Co-IP was performed with purified anti-NS1 antibodies as indicated in Methods. The eluted samples were subjected to Western blotting with anti-NS1 and anti-NS5 antibodies, as indicated. (b) BHK and DF-1 cells were infected with the viruses used in (a). PBS was used as a control. Co-IP was performed with purified anti-NS5 antibodies as indicated in Methods. The eluted samples were subjected to Western blotting by anti-NS5 antibodies and anti-NS1 antibodies, as indicated. The numbers below lanes in (a) indicate the relative intensity of the NS1′ or NS5 band divided by the intensity of the NS1 band. The numbers below lanes in (b) indicate the relative intensity of the NS1 or NS1′ band divided by the intensity of the NS5 band.

propagation (Melian *et al.*, 2010; Winkelmann *et al.*, 2011; Ye *et al.*, 2012). A recent report demonstrated that NS1′ and NS1 are co-localized in viral RNA replication sites in infected cells, that NS1′ can complement for the deleted NS1 during virus replication and that there is no significant difference in the efficiency of complementation between NS1 and NS1′ (Young *et al.*, 2013). In the present report, it was demonstrated that NS1′ protein facilitated virus production based on the increasing viral RNA level in avian cells (Figs 2 and 6). An NS1′-induced increase in virus production and mortality of the ECEs was observed (Fig. 7). It was also demonstrated that NS1′ was expressed more efficiently in avian DF-1 cells (Fig. 1c) than in BHK cells, which were used in previous reports (Melian *et al.*, 2010; Winkelmann *et al.*, 2011; Ye *et al.*, 2012). NS1′ expression and growth characteristics in porcine kidney cells (PS cells) and Green monkey kidney cells (Vero cells) were similar with those in BHK cells (Fig. S3). These findings suggest that NS1′ plays a crucial role in RNA synthesis and production of JEV, especially in avian cells.

The results of this study also provide some noteworthy insights on NS1′ molecular functions. First, NS1′ expression was three to four times higher in DF-1 cells than in mammalian cells (Figs 1c and S3a). Ribosomal frameshifting is a translational mechanism used by many viruses to co-ordinately express two proteins from a single mRNA at a defined ratio (Brierley *et al.*, 2007). It has been reported that the species from which ribosomes are derived could influence the frequency of frameshifting (Matsufuji *et al.*, 1996), and a different structure of different ribosomes could influence −1 ribosomal frameshifting efficiencies (Plant & Dinman, 2006). Birds and mammals may have a different translational mechanism regarding the −1 ribosomal frameshifting, and the higher ratio of NS1′ translation could occur in avian cells. Secondly, quantitative RT-PCR analysis revealed that NS1′ increased viral

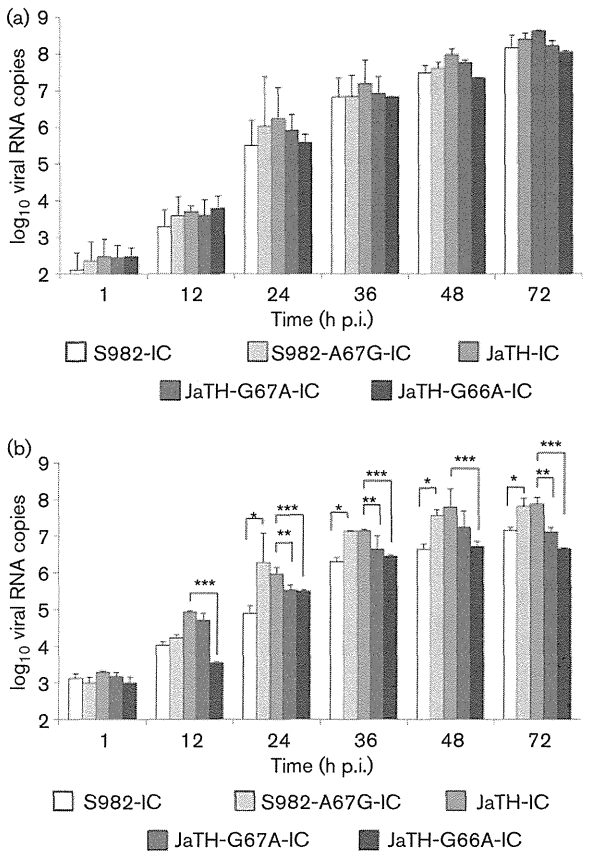

Fig. 6. Viral RNA level in BHK and DF-1 cells. Viral RNA copies from cell lysates were measured by real-time quantitative RT-PCR. (a, b) BHK (a) and DF-1 (b) cells were infected with the indicated viruses at an m.o.i. of 0.1. Viral RNA copies were measured at the indicated times p.i. The values were normalized to expression of β-actin and glyceraldehyde 3-phosphate dehydrogenase (GAPDH) for mouse and avian cells, respectively. The values between two groups were tested by Student's *t*-test or Welch test analysis. Asterisks indicate statistical significance between viruses at $P<0.05$: *, S982-IC versus S982-A67G-IC; **, JaTH-IC versus JaTH-G67A-IC; ***, JaTH-IC versus JaTH-G66A-IC. Results are expressed as means ± SD from three independent experiments.

RNA copy number in DF-1 cells but not in BHK cells (Fig. 6). A higher co-localization rate and effective interactions were also shown to occur between NS1′ and NS5 proteins in avian cells (Figs 4 and 5). These results indicate that the efficient interaction of NS1′ and NS5 may influence effective viral RNA replication in avian cells. In future studies, the role of NS1′ in replication could be elaborated further by a complementation assay (Young *et al.*, 2013). Thirdly, the NS1′-expressing viruses increased virus production and mortality rate in ECEs (Fig. 7). The present study reports for the first time the characteristic effects of JEV infection in ECEs. It will be important to reveal in future investigations how NS1′ expression affects viral pathogenicity, and the duration of a higher viraemia titre in adult birds. In JEV natural transmission, over 90 bird species are known to be amplification and reservoir hosts of JEV, and they represent the primary effective animal hosts because they can be highly viraemic and can be an outstanding source of infection for mosquitoes (Le Flohic *et al.*, 2013). Over long distances, migratory birds are the most likely spreader of JEV because some have a complex migration system over a large geographical area (van den Hurk *et al.*, 2009). Based on these situations, adaptation to birds provides a good advantage for JEV survival, and the NS1′-expressing virus showed higher fitness in avian cells (Fig. S4).

In conclusion, this study indicates that one of the intrinsic functions of the NS1′ protein found to be specific for avian cells and tissues is to facilitate virus production. The NS1′ protein works efficiently with NS5 proteins and increases viral RNA synthesis. This suggests a possible important role for NS1′ in reservoir birds by contributing to the survival of JEV through the retention of sufficient amounts of virus during the natural cycles by facilitating virus production in avian hosts.

METHODS

Cells and viruses. Baby hamster kidney (BHK) and chicken embryonic fibroblast (DF-1) cells were maintained in minimum essential medium (MEM) with 10 % FCS and 0.2 mM non-essential amino acids. BHK and DF-1 cells were allowed to grow at 37 °C with 5 % CO_2. JEV strain JaOArS982 was isolated from a *Culex* mosquito pool in Osaka, Japan, in 1982 (Sumiyoshi *et al.*, 1987). JEV strain JaTH160 was isolated from a human brain in Tokyo, Japan, in 1960 (Fujii *et al.*, 2008). Following a procedure described previously (Hayasaka *et al.*, 2004; Morita *et al.*, 2001), full-length JEV cDNA ICs designated S982-IC and JaTH-IC were constructed (Takamatsu *et al.*, unpublished data).

Mutagenesis of ICs. Site-directed mutagenesis was introduced as described previously (Yu *et al.*, 2007a) to substitute an A with a G at nt 67 of the *NS2A* gene (A67G) in the IC S982-IC, and a G with an A at nt 66 and 67 of the *NS2A* gene (G66A and G67A, respectively) in the other clone JaTH-IC. The primers used for mutagenesis are indicated in Table S2. The sequences of recovered viruses were confirmed and the resulting mutated viruses were designated S982-A67G-IC, JaTH-G67A-IC and JaTH-G66A-IC, respectively. It has been reported that the nucleotide change from G to A at nt 66 of the *NS2A* gene abolishes NS1′ expression in JEV (Ye *et al.*, 2012). In order to eliminate the influence of the amino acid change from I to V at aa 23 of the *NS2A*, JaTH-G66A-IC was developed. The experimental protocols were approved by the committee for recombinant DNA experiments, Nagasaki University, Japan (approval number: 0909021017).

Recovery of infectious virus. Full-length cDNA clones were linearized and transcribed into RNA using an SP6 transcription system as described previously (Hayasaka *et al.*, 2004), and the RNA was introduced into BHK cells by electroporation (Hayasaka *et al.*, 2004). The full-length cloned viruses were propagated in BHK cells to generate working stocks, and these virus stocks were stored at −80 °C.

Growth curves in BHK and DF-1 cells. JEV infection was performed on a monolayer of cells on 24-well plates at an m.o.i. of 0.1. After incubation for 60 min, the virus inoculum was removed and the cells were washed twice with PBS. Medium (0.5 ml) was added to each well and the plates were incubated at 37 °C under 5 %

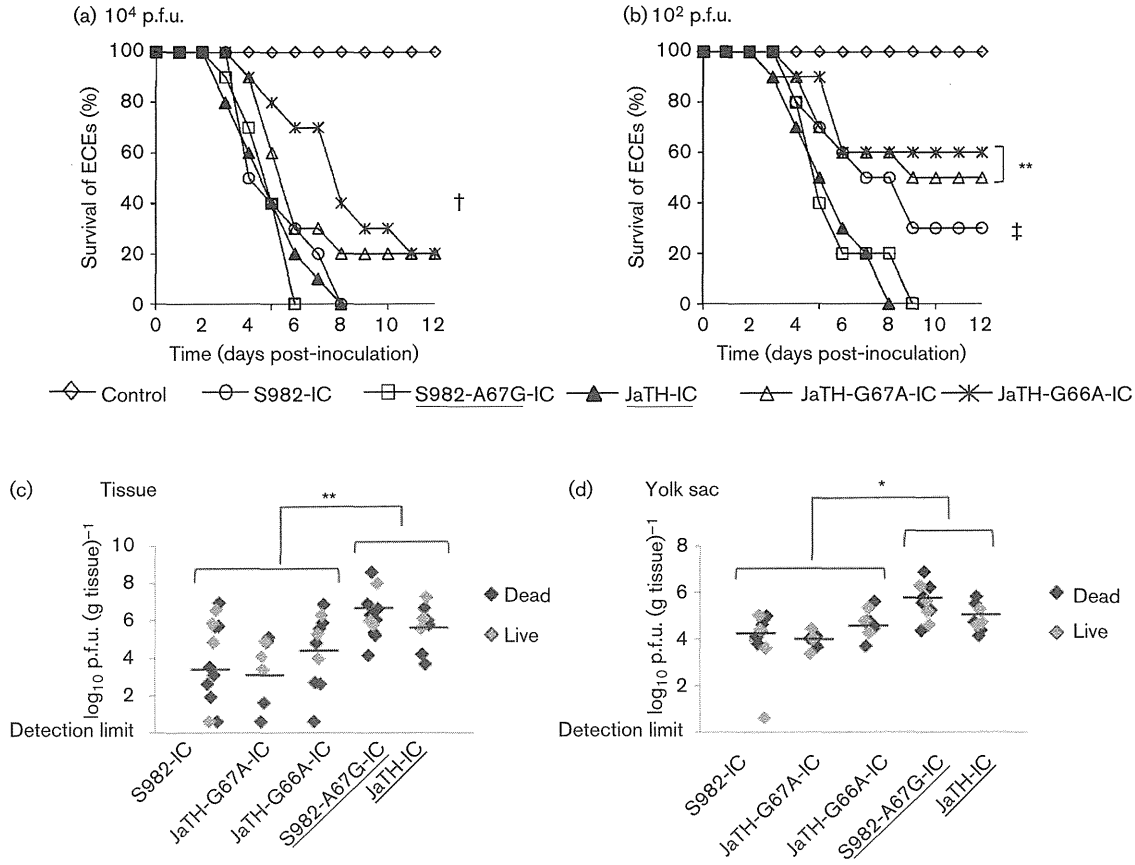

Fig. 7. Survival curves and virus titres from tissues of live and dead ECEs. (a, b) Seven-day-old ECEs (n=10) were inoculated by the indicated viruses at a titre of 10^4 p.f.u. per egg (a) or 10^2 p.f.u. per egg (b). Survival was monitored daily until 12 days post-inoculation. A log-rank test was performed to compare survival curves of JEV-inoculated ECEs. †, Significant difference between the survival curves of ECEs infected with the NS1′-expressing viruses (S982-A67G-IC and JaTH-IC) and JaTH-G66A-IC (P<0.05); ‡, significant difference between the survival curves of ECEs infected with the NS1′-expressing viruses and S982-IC (P<0.05); **, significant difference between the survival curves of ECEs infected with the NS1′-expressing viruses and the NS1′-non-expressing viruses (JaTH-G67A-IC and JaTH-G66A-IC) (P<0.01). (c, d) On day 5 post-inoculation, virus titres were determined from homogenized tissues of live (n=3–4) and dead (n=6–10) ECEs that had been inoculated with 10^4 p.f.u. per egg of the indicated viruses. The distribution of the virus titres from embryonic tissue samples (c) and from the yolk sac (d) was plotted. The values between two groups were tested by one-way ANOVA. Asterisks indicate statistical significance (*P<0.05; **P<0.01) in the difference of titres between the NS1′-expressing viruses and the NS1′-non-expressing viruses. Underlining indicates the NS1′-expressing viruses.

CO_2. The supernatants were harvested at 0, 24, 48 and 72 h p.i. and stored in aliquots at −80 °C prior to titration.

Focus formation and virus titration. Focus formation was performed on BHK and DF-1 cells as described previously (Espada-Murao & Morita, 2011). Virus titres were determined by plaque-forming assays on BHK cells and expressed as p.f.u. ml^{-1}. A 10-fold serial dilution of viral stocks was used for infection, and an overlay of MEM with 2 % FCS and 1 % methylcellulose was added after viral adsorption. Cells were incubated at 37 °C with 5 % CO_2 for 4 days, fixed with 4 % paraformaldehyde in phosphate buffer (WAKO) and stained with 0.1 % crystal violet in 10 % ethanol (Hayasaka *et al.*, 2009).

NS1′ antibody. NS1′ polyclonal antibodies were produced from C57BL/6j mice (Japan SLC Co.), which were injected with a peptide antigen (Fig. S5). The antigen was prepared following a procedure described previously (Yu *et al.*, 2007b). Here, the *NS1′* gene was amplified using primers 5′-AAAGGATCCTCAGCTGGGCCTTC-TGG-3′and 5′-AAACTCGAGTCAGTGTAAGTGATGCC-3′, with the underlined nucleotides indicating restriction sites. PCR-amplified DNA fragment was digested with *Bam*HI and *Xho*I and cloned into the corresponding restriction sites of pGEX6p1 (GE Healthcare). The plasmids were transformed into BL21 Codon Plus (Agilent). Transformed *Escherichia coli* cells were cultured in 500 ml Terrific Broth containing ampicillin at a concentration of 50 μg ml^{-1}. Production of the NS1′ protein was induced by the addition of 0.5 mM IPTG when the OD_{600} of the culture reached 0.5. After IPTG induction at 37 °C for 3 h, the cells were harvested by centrifugation and washed with PBS. The cell suspension was sonicated in 5 s pulses at 10 s intervals for 5 min and centrifuged at 20 000 *g* for 35 min.

Supernatants were collected and filtered through 0.45 μM filter (Millipore) and applied to a glutathione–Sepharose 4B column (GE Healthcare). After washing with PBS twice, the purified protein was eluted with 50 mM Tris/HCl (pH 8.0), 100 mM NaCl, 10 mM glutathione. Protein concentrations were determined by the Bradford method and purity was confirmed by SDS-PAGE as described previously (Yu *et al.*, 2005). Purified proteins were aliquotted and stored at −30 °C prior to injection. Mouse anti-NS1 and rabbit anti-NS5 polyclonal antibodies were prepared applying a procedure similar to that of the anti-NS1′ antibody production (Yu *et al.*, 2007a). The experimental protocols were approved by the Animal Care and Use Committee, Nagasaki University, Japan.

Confocal laser-scanning microscopy. JEV infection was performed on a monolayer of cells on eight-well chamber slides (Nunc) at an m.o.i. of 10. At 48 h p.i., the cells were subjected to immunostaining as described previously (Espada-Murao & Morita, 2011). Briefly, the cells were fixed with 2 % paraformaldehyde, permeabilized with 1 % NP-40, blocked and stained. The primary antibodies used were as follows: mouse anti-NS1, mouse anti-NS1′ and rabbit anti-NS5 polyclonal antibodies. Alexa Fluor 488-conjugated anti-rabbit and Alexa Fluor 568-conjugated anti-mouse antibodies (Invitrogen) were used for secondary labelling. Finally, the cells were incubated with DAPI for nuclear counterstaining. Images were captured using an LSM780 confocal laser-scanning microscope (Carl Zeiss).

Western blotting. JEV infection was performed on a monolayer of cells on 12-well plates at an m.o.i. of 10. At 48 h p.i., the cells were washed with PBS and resuspended in 100 μl lysis buffer [8 M urea, 500 mM Tris/HCl (pH 8.0), 2.5 mM EDTA]. After 30 min on ice, the cells were centrifuged at 20 000 *g* for 30 min at 4 °C. Each supernatant was mixed with acetone at a volume 10 times that of the supernatant and kept at −80 °C. The chilled samples were centrifuged under the same conditions as above and each supernatant was discarded. The pellets were mixed with SDS-PAGE sample buffer [62.5 mM Tris/HCl (pH 6.8), 4 % SDS, 10 % 2-mercaptoethanol, 0.1 % bromophenol blue] and then heated at 95 °C for 3 min. Equal volumes of samples were loaded onto a 10–20 % polyacrylamide gradient gel (e-PAGEL; ATTO) and separated by SDS-PAGE. Western blotting was performed as described previously (Okamoto *et al.*, 2012; Yu *et al.*, 2007a). For the primary antibody reaction, PVDF membranes (Millipore) were treated with mouse anti-β-actin (Santa Cruz Biotechnology, 1 : 1000 dilution), mouse anti-NS1 (1 : 250 dilution), mouse anti-NS1′ (1 : 250 dilution) or rabbit anti-NS5 (1 : 250 dilution) polyclonal antibodies. For the secondary antibody reaction, membranes were treated with the corresponding anti-mouse IgG–HRP (Santa Cruz Biotechnology, 1 : 10 000 dilution) or anti-rabbit IgG–HRP (Santa Cruz Biotechnology, 1 : 10 000 dilution). Protein bands were developed using Luminata Forte Western HRP Substrate (Millipore) and detected by using an LAS-4000 Mini Luminescent Image Analyzer (Fujifilm). The intensity of bands was calculated using ImageJ software (Schneider *et al.*, 2012).

Co-IP. The co-IP procedure was performed using protein A/G–Sepharose (GE Healthcare) with purified anti-NS1 or anti-NS5 polyclonal antibodies. JEV infection was performed on a monolayer of BHK and DF-1 cells in 150 cm^2 flasks. PBS was used in the control cells. At 48 h p.i., the cells were washed with cold PBS and lysed with 50 mM Tris/HCl (pH 7.5), 150 mM NaCl, 1 mM EDTA, 1 % NP-40 and protease inhibitor (Thermo Scientific). The lysed solutions were sonicated for 15–30 s and centrifuged at 12 000 *g* for 10 min. Supernatants were collected and subjected to co-IP according to the manufacturer's instructions. Briefly, after the antigen–antibody reaction had taken place at 4 °C for 1 h, protein A/G–Sepharose was added. After incubation at 4 °C overnight, the solutions were centrifuged at 12 000 *g* for 20 s and the pellets washed three times with wash buffer [50 mM Tris/HCl (pH 7.5), 50 mM NaCl, 1 mM EDTA, protease inhibitor]. Finally, elution was achieved through the use of SDS-PAGE sample buffer. Western blotting was carried out following the procedure above.

Real-time quantitative RT-PCR. JEV infection was performed on a monolayer of cells on 24-well plates at an m.o.i. of 0.1. At the indicated times, total RNA was harvested from cells using an RNeasy Mini kit (Qiagen). One microgram of RNA in a total volume of 20 μl was reverse transcribed with a Prime Script RT Reagent kit (TaKaRa) to obtain cellular mRNA and JEV RNA. Two microlitres of the product was used for real-time PCR (Applied Biosystems) with SYBR Premix Ex *Taq* II (TaKaRa). The number of copies of viral RNA, β-actin and glyceraldehyde 3-phosphate dehydrogenase (GAPDH) mRNAs was calculated by absolute quantification based on *in vitro*-transcribed JEV RNA, β-actin and GAPDH standards (Li *et al.*, 2013). The real-time RT-PCR primers are shown in Table S3.

Inoculation of ECEs. ECEs have been used for virus isolation and propagation (Clavijo *et al.*, 2000; Crespo *et al.*, 2009). Infection of ECEs with JEV in the present study was performed following the basic procedure used for WNV (Osorio *et al.*, 2012) and Crimean–Congo haemorrhagic fever virus (Xia *et al.*, 2013). Seven-day old ECEs were assigned per experimental or control group. These ECEs were inoculated with 200 μl viral inoculum (10^4 or 10^2 p.f.u. for experimental groups) or PBS (for control group) into the allantoic cavity, after which they were kept at 37 °C in an incubator. ECEs were candled once daily after inoculation to check their survival until 12 days post-inoculation. Dead ECEs in the first 24 h post-inoculation were discarded and the cause of their death was considered to be non-specific (Xia *et al.*, 2013).

Virus recovery from tissues and titration. Both dead and live ECEs at day 5 post-inoculation were chilled at 4 °C for 1 h in preparation for collecting tissues. The egg surface was disinfected with 70 % ethanol. The portion of the egg shell that covered the air cell was disinfected and a pair of sterile forceps was used to crack and remove the egg shell over the air cell. Embryonic tissues and yolk sac tissues were grasped with sterile forceps and stored in cryovials at −80 °C prior to titration. These samples were homogenized on a 70 μm cell strainer (BD Biosciences) with a particular volume (mg μl^{-1}) of medium. The virus titre in each sample was determined by a plaque-forming assay in BHK cells and expressed as p.f.u. (g tissue)$^{-1}$ (Hayasaka *et al.*, 2009).

ACKNOWLEDGEMENTS

We thank Dr Ichiro Kurane and Dr Tomohiko Takasaki from the National Institute of Infectious Diseases, Tokyo, Japan, for providing strain JaTH160; Dr Jiro Yasuda from the Department of Emerging Infectious Diseases, Institute of Tropical Medicine (NEKKEN), Nagasaki University, Nagasaki, Japan, for providing technical advice; and Mr Kotaro Aoki from the Department of Virology, Institute of Tropical Medicine (NEKKEN), Nagasaki University, Nagasaki, Japan, for providing technical assistance. This study was supported by a Grant-in-Aid for Scientific Research from the Ministry of Education, Culture, Sports, Science and Technology (MEXT), Japan, Young Researcher Overseas Visits Program for Vitalizing Brain Circulation, MEXT, Japan, the Global COE program, MEXT, Japan, the Japan Initiative for Global Network on Infectious Diseases (J-GRID), MEXT, Japan, and a Grant-in-Aid for Scientific Research from the Ministry of Health, Labour, and Welfare, Japan.

REFERENCES

Avirutnan, P., Fuchs, A., Hauhart, R. E., Somnuke, P., Youn, S., Diamond, M. S. & Atkinson, J. P. (2010). Antagonism of the

complement component C4 by flavivirus nonstructural protein NS1. *J Exp Med* **207**, 793–806.

Blitvich, B. J., MacKenzie, J. S., Coelen, R. J., Howard, M. J. & Hall, R. A. (1995). A novel complex formed between the flavivirus E and NS1 proteins: analysis of its structure and function. *Arch Virol* **140**, 145–156.

Brierley, I., Pennell, S. & Gilbert, R. J. (2007). Viral RNA pseudoknots: versatile motifs in gene expression and replication. *Nat Rev Microbiol* 5, 598–610.

Chen, L. K., Liao, C. L., Lin, C. G., Lai, S. C., Liu, C. I., Ma, S. H., Huang, Y. Y. & Lin, Y. L. (1996). Persistence of Japanese encephalitis virus is associated with abnormal expression of the nonstructural protein NS1 in host cells. *Virology* **217**, 220–229.

Chung, K. M., Liszewski, M. K., Nybakken, G., Davis, A. E., Townsend, R. R., Fremont, D. H., Atkinson, J. P. & Diamond, M. S. (2006a). West Nile virus nonstructural protein NS1 inhibits complement activation by binding the regulatory protein factor H. *Proc Natl Acad Sci U S A* **103**, 19111–19116.

Chung, K. M., Nybakken, G. E., Thompson, B. S., Engle, M. J., Marri, A., Fremont, D. H. & Diamond, M. S. (2006b). Antibodies against West Nile virus nonstructural protein NS1 prevent lethal infection through Fc γ receptor-dependent and -independent mechanisms. *J Virol* **80**, 1340–1351.

Chung, K. M., Thompson, B. S., Fremont, D. H. & Diamond, M. S. (2007). Antibody recognition of cell surface-associated NS1 triggers Fc-γ receptor-mediated phagocytosis and clearance of West Nile virus-infected cells. *J Virol* **81**, 9551–9555.

Clavijo, A., Heckert, R. A., Dulac, G. C. & Afshar, A. (2000). Isolation and identification of bluetongue virus. *J Virol Methods* **87**, 13–23.

Crespo, R., Shivaprasad, H. L., França, M. & Woolcock, P. R. (2009). Isolation and distribution of West Nile virus in embryonated chicken eggs. *Avian Dis* **53**, 608–612.

Espada-Murao, L. A. & Morita, K. (2011). Delayed cytosolic exposure of Japanese encephalitis virus double-stranded RNA impedes interferon activation and enhances viral dissemination in porcine cells. *J Virol* **85**, 6736–6749.

Ferreira, V. P., Pangburn, M. K. & Cortés, C. (2010). Complement control protein factor H: the good, the bad, and the inadequate. *Mol Immunol* **47**, 2187–2197.

Firth, A. E. & Atkins, J. F. (2009). A conserved predicted pseudoknot in the NS2A-encoding sequence of West Nile and Japanese encephalitis flaviviruses suggests NS1′ may derive from ribosomal frameshifting. *Virol J* **6**, 14.

Fujii, Y., Kitaura, K., Nakamichi, K., Takasaki, T., Suzuki, R. & Kurane, I. (2008). Accumulation of T-cells with selected T-cell receptors in the brains of Japanese encephalitis virus-infected mice. *Jpn J Infect Dis* **61**, 40–48.

Ghosh, D. & Basu, A. (2009). Japanese encephalitis – a pathological and clinical perspective. *PLoS Negl Trop Dis* **3**, e437.

Hayasaka, D., Gritsun, T. S., Yoshii, K., Ueki, T., Goto, A., Mizutani, T., Kariwa, H., Iwasaki, T., Gould, E. A. & Takashima, I. (2004). Amino acid changes responsible for attenuation of virus neurovirulence in an infectious cDNA clone of the Oshima strain of tick-borne encephalitis virus. *J Gen Virol* **85**, 1007–1018.

Hayasaka, D., Nagata, N., Fujii, Y., Hasegawa, H., Sata, T., Suzuki, R., Gould, E. A., Takashima, I. & Koike, S. (2009). Mortality following peripheral infection with tick-borne encephalitis virus results from a combination of central nervous system pathology, systemic inflammatory and stress responses. *Virology* **390**, 139–150.

Khromykh, A. A., Sedlak, P. L., Guyatt, K. J., Hall, R. A. & Westaway, E. G. (1999). Efficient trans-complementation of the flavivirus kunjin NS5 protein but not of the NS1 protein requires its coexpression with other components of the viral replicase. *J Virol* **73**, 10272–10280.

Le Flohic, G., Porphyre, V., Barbazan, P. & Gonzalez, J. P. (2013). Review of climate, landscape, and viral genetics as drivers of the Japanese encephalitis virus ecology. *PLoS Negl Trop Dis* **7**, e2208.

Li, Z., Wang, Y., Li, X., Li, X., Cao, H. & Zheng, S. J. (2013). Critical roles of glucocorticoid-induced leucine zipper in infectious bursal disease virus (IBDV)-induced suppression of type I Interferon expression and enhancement of IBDV growth in host cells via interaction with VP4. *J Virol* **87**, 1221–1231.

Lin, Y. L., Chen, L. K., Liao, C. L., Yeh, C. T., Ma, S. H., Chen, J. L., Huang, Y. L., Chen, S. S. & Chiang, H. Y. (1998). DNA immunization with Japanese encephalitis virus nonstructural protein NS1 elicits protective immunity in mice. *J Virol* **72**, 191–200.

Lindenbach, B. D. & Rice, C. M. (1997). *trans*-Complementation of yellow fever virus NS1 reveals a role in early RNA replication. *J Virol* **71**, 9608–9617.

Lindenbach, B. D. & Rice, C. M. (1999). Genetic interaction of flavivirus nonstructural proteins NS1 and NS4A as a determinant of replicase function. *J Virol* **73**, 4611–4621.

MacKenzie, J. M., Jones, M. K. & Young, P. R. (1996). Immunolocalization of the dengue virus nonstructural glycoprotein NS1 suggests a role in viral RNA replication. *Virology* **220**, 232–240.

Mason, P. W. (1989). Maturation of Japanese encephalitis virus glycoproteins produced by infected mammalian and mosquito cells. *Virology* **169**, 354–364.

Matsufuji, S., Matsufuji, T., Wills, N. M., Gesteland, R. F. & Atkins, J. F. (1996). Reading two bases twice: mammalian antizyme frameshifting in yeast. *EMBO J* **15**, 1360–1370.

Melian, E. B., Hinzman, E., Nagasaki, T., Firth, A. E., Wills, N. M., Nouwens, A. S., Blitvich, B. J., Leung, J., Funk, A. & other authors (2010). NS1′ of flaviviruses in the Japanese encephalitis virus serogroup is a product of ribosomal frameshifting and plays a role in viral neuroinvasiveness. *J Virol* **84**, 1641–1647.

Morita, K., Tadano, M., Nakaji, S., Kosai, K., Mathenge, E. G., Pandey, B. D., Hasebe, F., Inoue, S. & Igarashi, A. (2001). Locus of a virus neutralization epitope on the Japanese encephalitis virus envelope protein determined by use of long PCR-based region-specific random mutagenesis. *Virology* **287**, 417–426.

Muylaert, I. R., Chambers, T. J., Galler, R. & Rice, C. M. (1996). Mutagenesis of the N-linked glycosylation sites of the yellow fever virus NS1 protein: effects on virus replication and mouse neurovirulence. *Virology* **222**, 159–168.

Okamoto, K., Kinoshita, H., Parquet, M. C., Raekiansyah, M., Kimura, D., Yui, K., Islam, M. A., Hasebe, F. & Morita, K. (2012). Dengue virus strain DEN2 16681 utilizes a specific glycochain of syndecan-2 proteoglycan as a receptor. *J Gen Virol* **93**, 761–770.

Osorio, J. E., Ciuoderis, K. A., Lopera, J. G., Piedrahita, L. D., Murphy, D., Levasseur, J., Carrillo, L., Ocampo, M. C. & Hofmeister, E. (2012). Characterization of West Nile viruses isolated from captive American Flamingoes (*Phoenicopterus ruber*) in Medellin, Colombia. *Am J Trop Med Hyg* **87**, 565–572.

Plant, E. P. & Dinman, J. D. (2006). Comparative study of the effects of heptameric slippery site composition on −1 frameshifting among different eukaryotic systems. *RNA* **12**, 666–673.

Schlesinger, J. J. (2006). Flavivirus nonstructural protein NS1: complementary surprises. *Proc Natl Acad Sci U S A* **103**, 18879–18880.

Schneider, C. A., Rasband, W. S. & Eliceiri, K. W. (2012). NIH Image to ImageJ: 25 years of image analysis. *Nat Methods* **9**, 671–675.

Solomon, T. (2004). Flavivirus encephalitis. *N Engl J Med* **351**, 370–378.

Sumiyoshi, H., Mori, C., Fuke, I., Morita, K., Kuhara, S., Kondou, J., Kikuchi, Y., Nagamatu, H. & Igarashi, A. (1987). Complete nucleotide

sequence of the Japanese encephalitis virus genome RNA. *Virology* **161**, 497–510.

Sumiyoshi, H., Hoke, C. H. & Trent, D. W. (1992). Infectious Japanese encephalitis virus RNA can be synthesized from in vitro-ligated cDNA templates. *J Virol* **66**, 5425–5431.

van den Hurk, A. F., Ritchie, S. A. & MacKenzie, J. S. (2009). Ecology and geographical expansion of Japanese encephalitis virus. *Annu Rev Entomol* **54**, 17–35.

Westaway, E. G., Brinton, M. A., Gaidamovich, S. Ya, Horzinek, M. C., Igarashi, A., Kääriäinen, L., Lvov, D. K., Porterfield, J. S., Russell, P. K. & Trent, D. W. (1985). *Flaviviridae. Intervirology* **24**, 183–192.

Wilson, J. R., de Sessions, P. F., Leon, M. A. & Scholle, F. (2008). West Nile virus nonstructural protein 1 inhibits TLR3 signal transduction. *J Virol* **82**, 8262–8271.

Winkelmann, E. R., Widman, D. G., Suzuki, R. & Mason, P. W. (2011). Analyses of mutations selected by passaging a chimeric flavivirus identify mutations that alter infectivity and reveal an interaction between the structural proteins and the nonstructural glycoprotein NS1. *Virology* **421**, 96–104.

Xia, H., Zhao, J., Li, Y., Yin, S., Tang, S., Zhang, Z., Yu, J., Kou, Z., Fan, Z. & Li, T. (2013). Infection and propagation of Crimean-Congo hemorrhagic fever virus in embryonated chicken eggs. *Virus Res* **173**, 344–349.

Ye, Q., Li, X. F., Zhao, H., Li, S. H., Deng, Y. Q., Cao, R. Y., Song, K. Y., Wang, H. J., Hua, R. H. & other authors (2012). A single nucleotide mutation in NS2A of Japanese encephalitis-live vaccine virus (SA14-14-2) ablates NS1′ formation and contributes to attenuation. *J Gen Virol* **93**, 1959–1964.

Youn, S., Li, T., McCune, B. T., Edeling, M. A., Fremont, D. H., Cristea, I. M. & Diamond, M. S. (2012). Evidence for a genetic and physical interaction between nonstructural proteins NS1 and NS4B that modulates replication of West Nile virus. *J Virol* **86**, 7360–7371.

Young, L. B., Melian, E. B. & Khromykh, A. A. (2013). NS1′ colocalizes with NS1 and can substitute for NS1 in West Nile virus replication. *J Virol* **87**, 9384–9390.

Yu, F., Le, M. Q., Inoue, S., Thai, H. T., Hasebe, F., Del Carmen Parquet, M. & Morita, K. (2005). Evaluation of inapparent nosocomial severe acute respiratory syndrome coronavirus infection in Vietnam by use of highly specific recombinant truncated nucleocapsid protein-based enzyme-linked immunosorbent assay. *Clin Diagn Lab Immunol* **12**, 848–854.

Yu, F., Hasebe, F., Inoue, S., Mathenge, E. G. & Morita, K. (2007a). Identification and characterization of RNA-dependent RNA polymerase activity in recombinant Japanese encephalitis virus NS5 protein. *Arch Virol* **152**, 1859–1869.

Yu, F., Le, M. Q., Inoue, S., Hasebe, F., Parquet, M. C., Morikawa, S. & Morita, K. (2007b). Recombinant truncated nucleocapsid protein as antigen in a novel immunoglobulin M capture enzyme-linked immunosorbent assay for diagnosis of severe acute respiratory syndrome coronavirus infection. *Clin Vaccine Immunol* **14**, 146–149.

【原著】

Inhibitory effects of JNK on *Aedes albopictus* early larval development

Tomomitsu SATHO[1)], Yuki NAGANO[1)], Yuki ESHITA[2)], Yujin HISATOMI[1)], Akira SAKATA[1)], Takeshi MIYATA[1)], Nobuhiro KASHIGE[1)], Fumio MIAKE[1)], Lucky R RUNTUWENE[2)], Shuetsu FUKUSHI[3)], Masayuki SAIJYO[3)], Ichiro KURANE[3)], Shigeru MORIKAWA[3)] and Tetsuya MIZUTANI[3)]*

[1)]Microbiology Laboratory, Faculty of Pharmaceutical Sciences, Fukuoka University; 8-19-1 Nanakuma, Jonan-ku, Fukuoka 814-0180, Japan
[2)]Department of Infectious Disease Control, Faculty of Medicine, Oita University; 1-1 Idaigaoka, Hasama-machi, Oita 879-5593, Japan
[3)]Research and Education Center for Prevention of Global Infectious Diseases of Animals, Tokyo University of Agriculture and Technology; 3-5-8 Saiwaicho, Fuchu city, Tokyo 183-8509, Japan. Virology 1, National Institute of Infectious Diseases; 4-7-1 Gakuen, Musashimurayama, Tokyo 208-0011, Japan

ヒトスジシマカ若齢幼虫の成長に対するJNKの阻害効果

佐藤 朝光[1)], 長野 佑基[1)], 江下 優樹[2)], 久富 祐人[1)], 坂田 晃[1)], 宮田 健[1)], 鹿志毛 信広[1)], 見明 史雄[1)], Lucky R RUNTUWENE[2)], 福士 秀悦[3)], 西條 政幸[3)], 倉根 一郎[3)], 森川 茂[3)], 水谷 哲也[3)]*

[1)]福岡大学薬学部微生物薬品化学教室 〒814-0180 福岡市城南区七隈 8-19-1
[2)]大分大学医学部感染予防医学講座 〒879-5593 大分県由布市挾間町医大ヶ丘 1-1
[3)]東京農工大学 農学部附属国際家畜感染症防疫研究教育センター 〒183-8509 東京都府中市幸町 3-5-8
国立感染症研究所ウイルス第1部 〒208-0011 東京都武蔵村山市学園 4-7-1

Abstract

The regulation of mitogen-activated protein kinase (MAPK) during the growth of early instar mosquito larvae has not been determined. In this study, we exposed early first instar *Aedes* mosquito larvae to three MAPK inhibitors (SP600125, SB203580, and PD98059). *Aedes* first instar larvae were exposed to siRNA targeted against the JNK signal transducer (JNK-siRNA). Higher larval mortality was observed after exposure to SP600125 (an inhibitor of c-Jun N-terminal protein kinase; JNK) than after treatment with the other two inhibitors. Exposure to JNK-siRNA significantly increased larval mortality at 48 h after exposure. These results suggest that the inhibition of JNK suppresses the growth of *Aedes* mosquitoes during their early larval development.

摘 要

蚊の若齢幼虫の成長におけるマイトジェン活性化プロテインキナーゼ（MAPK）の制御については明らかになっていない．本研究では，*Aedes* 属の蚊（ヤブカ）の幼虫に3種のMAPK阻害物質（SP600125, SB203580, PD98059），およびJNK（c-Jun N-terminal kinase）をターゲットにしたsiRNA（JNK-siRNA）を暴露させた．SP600125は他の2種の阻害物質に暴露させた場合よりも，幼虫の死亡率が高かった．一方，JNK-siRNAに暴露させると，幼虫の死亡率が有意に高まった．これらの結果は，JNKの阻害が，幼虫の発生初期のヤブカの成長を抑制することを示唆している．

Key words: *Aedes* mosquito (*Aedes* 属の蚊), larval development (幼虫発育), JNK

Introduction

The mitogen-activated protein kinase (MAPK) cascade is an intracellular signal transduction pathway that is evolutionally conserved and includes various members of the serine/threonine protein kinase family. In mammals, the MAPK cascade is comprised of at least four signal transduction pathways: c-Jun N-terminal protein kinase (JNK), extracellular signal-regulated protein kinase (ERK) 1/2, ERK5, and p38 (Hengartner, 2000). In particular, the

* Address correspondence and reprint requests to Tetsuya Mizutani. Tel/Fax: +81-42-367-5749, +81-42-367-5742, E-mail: tmizutan@cc.tuat.ac.jp
受付：2011年7月26日 (Received : 26 July, 2011)
受理：2012年2月1日 (Accepted : 1 February, 2012)

mammalian JNK signal transduction pathway plays an important role in its development.

The whole genome sequence of *Drosophila melanogaster* was determined, and the proteins encoded by this genome were compared with those encoded by the human genome. In addition, it was indicated that the number of apoptosis-related proteins is greater in vertebrates, suggesting that they possess a more complex mechanism of development (Aravind et al., 2001). For example, the genes *jnk1*, *jnk2*, and *jnk3* have been confirmed in mammalian cells, whereas *Drosophila* possesses only one JNK protein, which is encoded by the *basket* gene (Kanda and Miura, 2004). Furthermore, this comparison of genome sequences indicated that tumor necrosis factor (TNF) and the TNF receptor (TNFR) superfamily are present in both humans and *Drosophila* (Aravind et al., 2001). Eiger, which is a TNFR found in *D. melanogaster*, modifies the morphogenesis of *Drosophila* compound eyes and wings through JNK (Moreno et al., 2002).

Mosquitoes are the most important vectors of arboviruses and malarial parasites. In view of their medical importance, mosquitoes have been the focus of considerable molecular biological research. However, there have been few studies regarding the mosquito MAPK cascade, and its precise function remains largely unknown in development.

Aedes albopictus is highly susceptible to infection with West Nile virus (WNV) (Turell et al., 2001; Sardelis et al., 2002). Indeed, WNV has been isolated from *Ae. albopictus* collected in the field (Holick et al., 2002). This suggests that *Ae. albopictus* is a vector of WNV. One of the mechanisms by which WNV is taken up into the cells of *Ae. albopictus* is endocytosis (Mizutani et al., 2003a; Chu et al., 2006), and endocytosis and phagocytosis are both regulated by JNK (Mizutani et al., 2003a). The nucleotide sequence of JNK isolated from the *Ae. albopictus* C6/36 cell line was determined (Mizutani et al., 2003b).

In common with mammalian and *Drosophila* JNK, mosquito JNK is suspected to play a key role in development. This study was examined whether inhibition of mosquito MAPK cascade, including JNK, affects the growth of early instar larvae using MAPK inhibitors and RNA interference (RNAi) techniques.

Materials and Methods

1. Mosquitoes

In this study, the *Aedes albopictus* Nagasaki colony and *Aedes aegypti* Tanzania colony were used. These two colonies were obtained from the Department of Vector Ecology & Environment, Institute of Tropical Medicine, Nagasaki University, Japan, and maintained in the insectary (controlled at 27 ± 1.0℃ and 70% ± 10% RH.) of the Microbiology Laboratory, Faculty of Pharmaceutical Sciences, Fukuoka University, Japan. The rearing density of the larvae was *ca.* 100 larvae/L, and they were kept in plastic trays (27 cm × 36 cm × 6 cm). As larval food, a 1:1 mixture of powdered mouse pellets (Clea Japan, Inc., Tokyo, Japan) and dried yeast (Tanabe Seiyaku Co., Ltd., Osaka, Japan) was supplied daily. After pupation, the pupae were collected and retained in water-filled plastic dishes (diameter, 90 mm; depth, 13 mm) in a screened cage (20 cm × 20 cm × 30 cm) until their eclosion. After all the adults had emerged, they were provided with a 3% sucrose solution as food. Mice were used for blood feeding to allow eggs to be harvested. All experiments were performed at 27 ± 1.0℃ and 70% ± 10% RH. under a 12:12 (L:D) photoperiod.

2. Bioassays

For the bioassays of the three MAPK inhibitors, early first instar *Aedes* larvae were transferred to each well of 96-well plates containing 200 μL of sterile purified water within 24 h of hatching (Nunc, Rochester, NY), and exposure experiments were performed as follows. PD98059, an inhibitor of the MEK upstream of ERK1/2; SB203580, a p38 inhibitor; and SP600125, a JNK inhibitor, were purchased from

Calbiochem Co., Ltd. (San Diego, CA). Each MAPK inhibitor was dissolved in dimethyl sulfoxide (DMSO; Wako Chemical Co., Ltd., Osaka, Japan) at a final concentration of 20 mM. The 20 mM solutions were then diluted to concentrations of 0.5 mM and 1 mM. Four mL aliquots of each dilution were added to the wells to give final exposure concentrations of 10 mM and 20 mM, respectively. In these MAPK inhibitor exposure experiments, five replicates per treatment were set up, each of which contained 24 larvae.

To examine the dose-dependent effects of exposure to SP600125, the 20 mM SP600125 solution was diluted to give seven concentrations (0.2, 0.3, 0.4, 0.5, 0.6, 0.8, and 1 mM). Four mL aliquots of each dilution were added to the wells (final exposure concentrations: 4 to 20 mM). In this bioassay, five replicates—each of which contained 24 larvae—were set up for each concentration. In all MAPK inhibitor exposure experiments, 4 mL of DMSO were added as a control.

In addition, the early first instar *Ae. albopictus* larvae were exposed to small interfering RNA (siRNA) targeting JNK (Table 1). The synthesized siRNA (JNK-siRNA) was designed based on a 94–113 bp nucleotide sequence of the JNK mRNA from the *Ae. albopictus* C6/36 cell line (accession number: AF515780). Another siRNA (scrambled-siRNA), which was not homologous to any arthropod gene sequence, including those of mosquitoes, was synthesized as a control. These two siRNA were purchased from Nippon E.G.T. Co., Ltd. (Toyama, Japan). Freeze-dried siRNA was dissolved using RNase-free water in 1.5 mL sample tubes (20 mM). The siRNA solutions (56.5 mL) were dispensed into each well along with RNase-free water at a final volume of 100 mL (concentration of siRNA: 11.3 mM). Finally, a single first instar larva was transferred into each well. Ten larvae were used in each of the five replicates. RNase-free water (56.5 mL) was used as a control.

After the exposure, food was supplied daily, and the 96-well microplates were placed in a controlled incubator set at 27 ± 1.0℃ and 70% ± 10% R.H. under a 12:12 (L:D) photoperiod. The larval instars were determined every 24 h based on the presence of cast-off larval skins and size.

3. Statistical analysis

Number of death of the first instar larvae was counted and the mortality rate of the first instar larvae (mean and standard error) was calculated for each replication, after correcting the data using Abbott's formula. The significance of the difference between mortality rates was analyzed according to Zar's method (Zar, 1984). The inhibitory effect of SP600125 was determined by the IC_{50} (inhibitory concentration 50%) value, which was estimated by probit analysis.

Results

The early first instar larvae from the two *Aedes* mosquito colonies were exposed to MAPK inhibitors, and their mortality rates were determined at 144 h after their exposure (Fig. 1). When the *Ae. albopictus* larvae were exposed to 10 mM and 20 mM SP600125 their mortality

Table 1. Synthesized siRNA used for bioassay against early first instar larvae of the *Aedes albopictus* Nagasaki colony

siRNA	Sequences
JNK-siRNA	5' GCAGAAUGUCGCCAUCAAATT 3' 3' TTCGUCUUACAGCGGUAGUUU 5'
Scrambled-siRNA	5' ACUCUAGGUCGCUUAGUUGTT 3' 3' TTUGAGAUCCAGCGAAUCAAC 5'

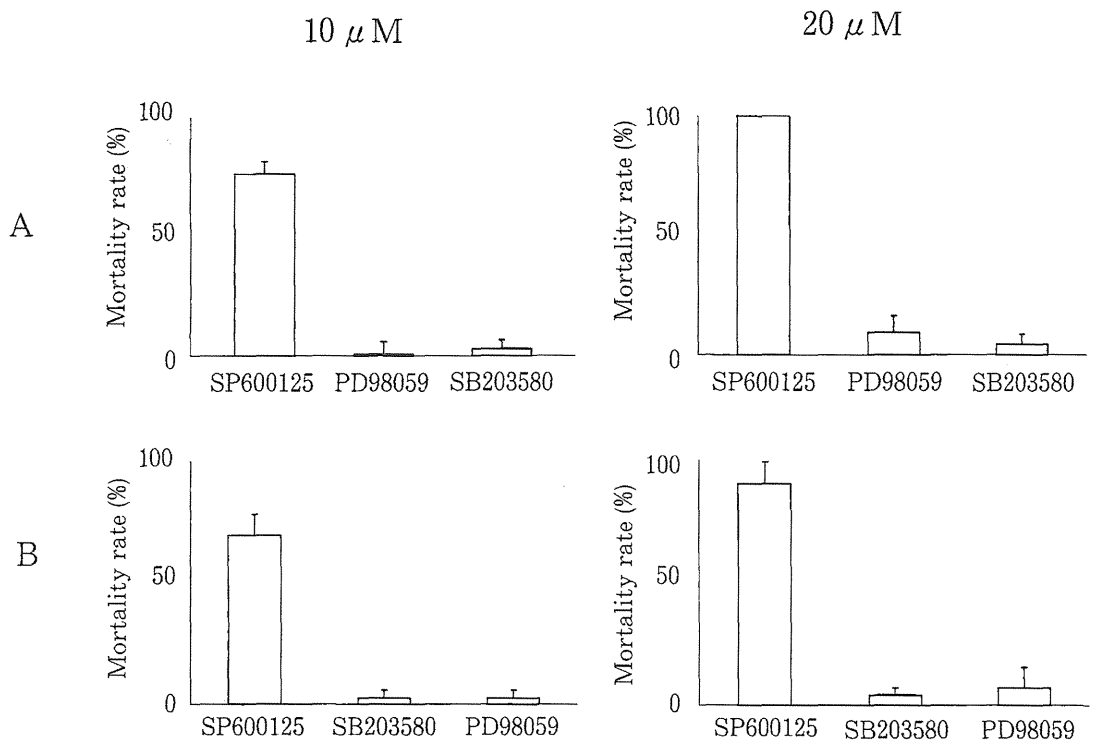

Fig. 1 Mortality rates of *Aedes* mosquito first instar larvae exposed to three MAPK inhibitors. A and B indicate the mortality rates of the first instar larvae of the *Aedes albopictus* Nagasaki colony and *Aedes aegypti* Tanzania colony, respectively.

rates were 91.6% ± 2.9% and 100% ± 0%, respectively (Fig. 1A). The mortality rates resulting from exposure to PD98059 and SB203580 were 0.9% ± 3.3% and 3.5% ± 1.3% at 10 mM and 9.4% ± 2.4% and 4.4% ± 1.6% at 20 mM, respectively (Fig. 1A). The mortality rate resulting from exposure to SP600125 was significantly higher than those associated with exposure to PD98059 or SB203580 ($P < 0.05$). There was no significant difference in the mortality rate between the larvae exposed to PD98059 and those exposed to SB203580 ($P < 0.05$).

On the other hand, when first instar *Ae. aegypti* larvae were exposed to 10 mM and 20 mM MAPK inhibitors, the mortality rates resulting from exposure to SP600125 were 69.2% ± 4.3% and 90.0% ± 4.5%, respectively (Fig. 1B). The mortality rates resulting from exposure to PD98059 and SB203580 were 2.5% ± 1.7% and 2.5% ± 1.3% at 10 mM and 4.2% ± 1.3% and 6.8% ± 4.0% at 20 mM, respectively. Similar to *Ae. albopictus* larvae, the mortality rate observed after exposure to SP600125 was significantly higher than those resulting from exposure to PD98059 or SB203580 ($P < 0.05$). The mortality rate resulting from exposure to PD98059 was not significantly different from that resulting from exposure to SB203580 ($P < 0.05$).

Subsequently, we assessed the dose dependency of the effects of SP600125 on the early first instar larvae from the two *Aedes* mosquito colonies (Table 2). As a result, we found that there were no significant differences between the regression lines of the mortality rates of the two colonies ($P < 0.05$). The IC_{50} values of SP600125 for *Ae. albopictus* and *Ae. aegypti* were 14.7 mM and 21.7 mM, respectively.

Next, early first instar *Ae. albopictus* larvae were exposed to siRNA targeting JNK, and the mortality rate of first instar larvae was calculated at 48 h (Fig. 2). In control, death larva was not observed and approximately 77% of larvae grew to second instar (Fig. 2). On the other hand, the mortality rate of the early first instar

Table 2. Regression lines and IC_{50} values for *Aedes* mosquito first instar larvae exposed to SP600125

Name of mosquito colony	Regression lines	IC_{50} (μM)
Aedes albopictus Nagasaki	Y = 2.59 log (X) + 1.98	14.7
Aedes aegypti Tanzania	Y = 1.91 log (X) + 2.44	21.7

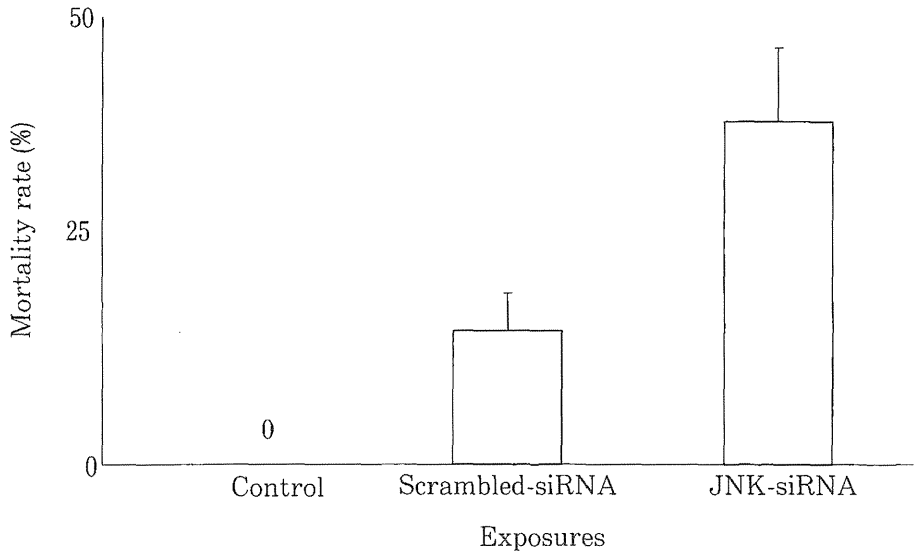

Fig. 2 Mortality rate of the first instar larvae of the *Aedes albopictus* Nagasaki colony at 48 h after exposure of synthesized siRNA-targeting JNK.

larvae increased rapidly by exposure of JNK-siRNA. In particular, difference in mortality rates resulting from exposure of JNK-siRNA and scrambled-siRNA at 48 h was significant (38.3% ± 8.3% and 15.0% ± 4.3%, respectively, $P < 0.05$).

Discussion

Among the *Aedes* mosquito larvae exposed to the three MAPK inhibitors (SP600125, PD98059, and SB203580) the highest mortality rate was detected among the early first instars exposed to SP600125. In addition, the mortality rates for both *Aedes* species exposed to SP600125 increased dose-dependently, although there was no significant difference between the IC_{50} values for the two colonies. These results suggest that mosquito JNK is one of the MAPKs that relate to growth in *Aedes* mosquito first instar larvae and that the activation of mosquito JNK is required during their early larval development. In *Drosophila*, JNK regulates in many metamorphosis events. For example, the loss of JNK activity alters the adhesion properties of larval cells and leads to the detachment of the imaginal and larval tissues during thorax closure in *Drosophila*, resulting phenotypic effects suppressing closure (Martin-Blanco et al., 2009). As well as *Drosophila* JNK, mosquito JNK might also regulate various metamorphosis events and abnormal metamorphosis, which is induced by the inactivation of JNK, might have led to the death of the first instar larvae exposed to the JNK inhibitors in the present study.

The microinjection of dsRNA, siRNA, or viral vectors has been reported to suppress the expression of target proteins in mosquitoes in a se-

quence-specific manner (Travanty et al., 2004; Boisson et al., 2006). Therefore, to confirm the role of JNK in the growth of *Aedes* mosquito first instar larvae, we exposed the larvae to siRNA targeting JNK. In this experiment, the exposure of *Aedes* larvae to the mosquito JNK siRNA resulted in a rapid elevation in their mortality rate after 48 h of exposure. Similarly, in the C6/36 cell line, a double-stranded RNA against GFP suppressed its protein expression at 48 h after transfection (Travanty et al., 2004), suggesting that exposure to siRNA targeting JNK inhibits the expression of JNK in the first instar larvae at 48 h.

This is the first report to show that, mosquito JNK, a mosquito MAPK, plays an important role in growth during early first instar larval development.

Acknowledgements

We thank Dr. Masahiro Takagi (Nagasaki University, Japan) for his helpful suggestions. This study was supported by Grants-in-Aid for Scientific Research (B) from Japan Society for the Promotion of Science (JSPS KAKENHI; 19380179 for TM and 20401050 for YE), Grant-in-Aid for Scientific Research (C) from JSPS (23590803 for YE), and the Ministry of Health, Labour, and Welfare, Japan (H23-SHINKO-IPPAN-010 for YE).

References

1) Aravind, L., Dixit, V. M., & Koonin, E. V. (2001) Apoptotic molecular machinery: vastly increased complexity in vertebrates revealed by genome comparisons. *Science* 291: 1279–1284.
2) Boisson, B., Jacques, J. C., Choumet, V., Martin, E., Xu, J., Vernick, K., Bourgouin, C. (2006) Gene silencing in mosquito salivary glands by RNAi. *FEBS Lett.* 580: 1988–1992.
3) Chu, J. J., Leong, P. W., Ng, & M. L. (2006) Analysis of the endocytic pathway mediating the infectious entry of mosquito-borne flavivirus West Nile into *Aedes albopictus* mosquito (C6/36) cells. *Virology* 349: 463–475.
4) Hengartner, M. O. (2000) The biochemistry of apoptosis. *Nature* 407: 770–776.
5) Holick, J., Kyle, A., Ferraro, W., Delaney, R. R., & Iwaseczko, M. (2002) Discovery of *Aedes albopictus* infected with West Nile virus in southeastern Pennsylvania. *J. Am. Mosq. Control Assoc.* 18: 131.
6) Kanda, H. & Miura, M. (2004) Regulatory roles of JNK in programmed cell death. *J. Biochem.* 136: 1–6.
7) Martin-Blanco, E., Pastor-Pareja, JC., & Garcia-Bellido, A. (2000) JNK and decapentaplegic signaling control adhesiveness and cytoskeleton dynamics during thorax closure in *Drosophila. Proc Natl Acad Sci U S A* 97: 7888–7893.
8) Mizutani, T., Kobayashi, M., Eshita, Y., Shirato, K., Kimura, T., Ako Y., Miyoshi, H., Takasaki, T., Kurane, I., Kariwa, H., Umemura, T., & Takashima, I. (2003a) Involvement of the JNK-like protein of the *Aedes albopictus* mosquito cell line, C6/36, in phagocytosis, endocytosis and infection of West Nile virus. *Insect Mol. Biol.* 12: 491–499.
9) Mizutani, T., Kobayashi, M., Eshita, Y., Inanami, O., Yamamori, T., Goto, A., Ako, Y., Miyoshi, H., Miyamoto H., Kariwa, H., Kuwabara, M., & Takashima, I. (2003b) Characterization of JNK-like protein derived from a mosquito cell line, C6/36. *Insect Mol. Biol.* 12: 61–66.
10) Moreno, E., Yan, M., & Basler, K. (2002) Evolution of TNF signaling mechanisms: JNK-dependent apoptosis triggered by Eiger, the *Drosophila* homolog of the TNF superfamily. *Curr. Biol.* 12: 1263–1268.
11) Sardelis, M. R., Turell, M. J., O'Guinn, M. L., Andre, R. G., & Roberts, D. R. (2002) Vector competence of three North American strains of *Aedes albopictus* for West Nile virus. *J. Am. Mosq. Control Assoc.* 18: 284–289.

12) Travanty, E. A., Adelman, Z. N., Franz, A. W., Keene, K. M., Beaty, B. J., Blair, C. D., James, A. A., & Olson, K. E. (2004) Using RNA interference to develop dengue virus resistance in genetically modified *Aedes aegypti*. *Insect Biochem. Mol. Biol.* 34: 607–613.

13) Turell, M. J., O'Guinn, M. L., Dohm, D. J., & Jones, J. W. (2001) Vector competence of North American mosquitoes (Diptera: Culicidae) for West Nile virus. *J. Med. Entomol.* 38: 130–134.

14) Zar, J. H. (1984) Biostatistical Analysis. 718pp. Second ed. Prentice-Hall Inc., New Jersey.

Journal of Parasitology and Vector Biology Vol. 3(1), pp. 19-21, January 2011
Available online at http://www.academicjournals.org/JPVB
ISSN 2141-2510 ©2011 Academic Journals

Short Communication

Prevalence of Phasi Charoen virus in female mosquitoes

Yusuke Sayama[1,2], Yuki Eshita[3], Takuya Yamao[4], Miho Nishimura[4], Tomomitsu Satho[4], Raweewan Srisawat[5], Narumon Komalamisra[5], Yupha Rongsriyam[5], Kouji Sakai[1], Shuetsu Fukushi[1], Masayuki Saijo[1], Hitoshi Oshitani[2], Ichiro Kurane[1], Shigeru Morikawa[1] and Tetsuya Mizutani[1]*

[1]Virology 1, National Institute of Infectious Diseases, Gakuen 4-7-1, Musashimurayama, Tokyo 208-0011, Japan.
[2]Department of Virology, Tohoku University School of Medicine, 2-1 Seiryo-machi, Aoba-ku, Sendai, 980-8575, Japan.
[3]Department of Infectious Disease Control, Faculty of Medicine, Oita University, 1-1 Idaigaoka, Hasama, Yufu-shi, Oita 879-5593, Japan.
[4]Faculty of Pharmaceutical Sciences, Fukuoka University, 8-19-1, Nanakuma, Jonan-ku, Fukuoka 814-0180, Japan.
[5]Department of Medical Entomology, Faculty of Tropical Medicine, Mahidol University, 420/6 Ratchawithi Road, Bangkok 10400, Thailand.

Accepted 28 July, 2010

The authors previously characterized a partial nucleic acid sequence for a novel virus, Phasi Charoen virus (PhaV), which was isolated from *Aedes aegypti* larvae in Thailand, and PhaV appears to belong to the family *Bunyaviridae* based on phylogenetic analysis of amino acid sequences. In this study, we examined whether adult female mosquitoes in Thailand are infected by PhaV, and they found that over 20% of adult female mosquitoes were infected by PhaV. These viruses were genetically similar to strains. This result suggested a high prevalence of PhaV in adult female mosquitoes.

Key words: PhaV, bunyavirus, female mosquito, high prevalence.

INTRODUCTION

Arboviruses are biologically transmitted to vertebrate hosts by blood-feeding arthropod vectors, such as mosquitoes, biting flies and ticks. The surveillance of viral infection in mosquitoes depended on amplification by reverse transcription-polymerase chain reaction (RT-PCR). However, unknown virus is difficult to detect by PCR. The authors recently developed a rapid system for determination of viral nucleic acid sequences (RDV) for detecting unknown viruses (Mizutani et al., 2007; Kihara et al., 2007; Maeda et al., 2008; Yamao et al., 2009), and by this method they identified the novel virus Phasi Charoen virus (PhaV), which was isolated from *Aedes aegypti* larvae collected from the Phasi Charoen district of Thailand using C6/36 cells in previous study (Yamao et al., 2009). PhaV infects and replicates slowly in mosquito C6/36 cells. The previously characterized partial nucleic acid sequence for this virus and PhaV appears to belong to the family *Bunyaviridae* based on phylogenetic analysis of amino acid sequences. Members of the *Bunyaviridae* family are icosahedral enveloped viruses with a tripartite negative-sense RNA genome comprising small, medium and large segments, named according to their molecular sizes (Gonzalez-Scarano et al., 1991). Among the members of *Bunyaviridae* family, the mosquito-transmitted Rift Valley Fever Virus (RVFV) is important as a human pathogen. PhaV was not found to be infectious to mammalian Vero cells, even after 8 days of incubation (Yamao et al., 2009). However, we cannot discount the possibility that PhaV has non-pathogenic properties in mammalian. In addition, we did not investigate data regarding the infectivity of adult female, in which blood was taken from mammal. In this study, we examined whether adult female mosquitoes in Thailand are infected or not by PhaV.

Aedes aegypti specimens (77 adult females) were collected from houses of patients clinically diagnosed with dengue fever from the Bang Khun Thian, Bang Bon,

*Corresponding author. E-mail: tmizutan@nih.go.jp. Tel: +81-425-61-0711. Fax: +81-425-65-3315.